JOURNAL OF PROTEOMICS 73 (2010) 1694–1706

available at www.sciencedirect.com

ScienceDirect

www.elsevier.com/locate/jprot

Changes induced by two levels of cadmium toxicity in the 2-DE protein profile of tomato roots

Jorge Rodríguez-Celma, Rubén Rellán-Álvarez, Anunciación Abadía, Javier Abadía, Ana-Flor López-Millán*

Plant Nutrition Department, Aula Dei Experimental Station (CSIC), P.O. Box 13034, E-50080, Zaragoza, Spain

ARTICLE INFO

Article history:
Received 17 February 2010
Accepted 5 May 2010

Keywords:
Cadmium
Metabolism
Root
Tomato
Two-dimensional gel electrophoresis

ABSTRACT

Tomato is an important crop from nutritional and economical points of view, and it is grown in greenhouses, where special substrates and the use of recycled water imply an increased risk of Cd accumulation. We investigated tomato root responses to low (10 μM) and high (100 μM) Cd concentrations at the root proteome level. Root extract proteome maps were obtained by 2-DE, and an average of 121, 145 and 93 spots were detected in the 0, 10 and 100 μM Cd treatments, respectively. The low Cd treatment (10 μM) resulted in significant and higher than 2-fold changes in the relative amounts of 36 polypeptides, with 27 of them identified by mass spectrometry, whereas the 100 μM Cd treatment resulted in changes in the relative amounts of 41 polypeptides, with 33 of them being identified. The 2-DE based proteomic approach allowed assessing the main metabolic pathways affected by Cd toxicity. Our results suggests that the 10 μM Cd treatment elicits proteomic responses similar to those observed in Fe deficiency, including activation of the glycolytic pathway, TCA cycle and respiration, whereas the 100 μM Cd treatment responses are more likely due to true Cd toxicity, with a general shutdown of carbon metabolism and increases in stress related and detoxification proteins.

1. Introduction

Cadmium is highly toxic to plants and animals [1]. In particular, Cd toxicity in crops has become a serious problem, especially in developed countries. Cadmium is released into the environment by human activities such as mining, agricultural use of commercial fertilizers, sewage sludge, manure and lime and industrial activities that release air pollutants and effluents with high Cd concentrations [2,3]. Food chain contamination is the main Cd exposure risk for humans, and Cd taken up by plants is accepted to be the main source of Cd accumulation in foods [4]. Cadmium is suggested to cause damage even at very low concentrations, and healthy plants may contain Cd levels that are toxic for mammals [5].

In polluted soils, Cd is generally present as a free ion or in other soluble forms, and its mobility depends on pH and on the presence of chelating substances and other cations [6]. It is accepted that Cd is taken up by roots via Fe/Zn transporters because of the low metal specificity of these proteins. There is evidence that metal transporters from different families such as ZIP and Nramp are able to transport several divalent cations, including Cd [7,8]. Also, it has been described that a Ca

Abbreviations: ACN, Acetonitrile; GADPH, Glyceraldehyde 3-phosphate dehydrogenase; GDH, Glutamate dehydrogenase; GST, Glutathione S-transferase; HSP, Heat shock protein; KOBAS, KEGG orthology-based annotation system; MDAR, Monodehydroascorbate reductase; MDH, Malate dehydrogenase; PCs, Phytochelatins; PDH, Pyruvate dehydrogenase; PTMs, Post translational modifications; TCA, Tricarboxylic acid cycle.

* *Corresponding author*. Tel.: +34 976716056; fax: +34 976716145.
E-mail address: jabadia@eead.csic.es (J. Abadía).

1874-3919/$ – see front matter © 2010 Elsevier B.V. All rights reserved.
doi:10.1016/j.jprot.2010.05.001

transport mechanism could be involved in Cd uptake [9]. Little is known about the chemical form(s) in which this heavy metal is present in the xylem, although it has been suggested that it may be associated with organic acids [10].

Common symptoms of Cd toxicity in plants are a marked growth inhibition [11], leaf chlorosis and appearance of leaf necrotic spots [11,12]. Physiological effects of Cd toxicity in plants include changes in photosynthetic efficiency, respiration and transpiration [11–13] and alterations in nutrient homeostasis, including changes in Mn, K, Mg and Ca uptake rates [11,14] and a Cd-induced Fe deficiency [11,12]. At the cellular level, Cd toxicity is known to cause alterations such as membrane damage, disruption of electron transport, inhibition/activation of enzymes and interaction with nucleic acids [15,16]. Possible mechanisms by which these disorders are generated are an induction of oxidative stress and competition with other metals such as Zn, Fe, and Mn, which are cofactors of many enzymes [14,17]. One of the main Cd detoxification mechanisms in plant cells is the synthesis of phytochelatins (PCs) [18]. Phytochelatins have high affinity for heavy metals and the metal–PC complexes are transported and sequestered in vacuoles to avoid metal toxicity [19]. Information about other detoxification/tolerance mechanisms comes mainly from the study of Cd-hyperaccumulators [20] and Cd-tolerant plants [21], whereas less information is available in commercial crops such as tomato. These processes include metal complexation with organic acids, PCs, cysteine, metallothioneins and other low molecular weight thiols [18,22–25] and both cellular and subcellular compartmentation [22,26].

In recent years, proteomic profiling has been used to study the effects of Cd toxicity in plants in different scenarios. Changes in proteomic profiles induced by Cd toxicity have been described in *Arabidopsis thaliana* and barley cell cultures [27,28] and in spinach, barley, *Thlaspi caerulescens* and poplar leaves [29–33]. Most of the root proteomic studies published so far have focused in model species such as *A. thaliana* [34] and Cd-tolerant or hyperaccumulator species such as poplar, *T caerulescens* and *Brasica juncea* [31,32,35]. Also, two proteomic studies have described the protective effects conferred by mycorrhizal symbiosis to roots of Cd-exposed *Pisum sativum* and *Medicago truncatula* plants [36,37]. To our knowledge, just one study on Cd toxicity including a species of agronomical interest, rice, has been published so far [38].

Tomato is a very important crop from nutritional and economical points of view (FAOSTAT Database, http://faostat.fao.org/). A large part of this crop is grown in greenhouses, using special substrates and fertilization techniques involving reutilization of water, therefore implying a significant risk of heavy metal concentration increases [39]. We have recently studied changes in growth, metal accumulation and physiology in tomato plants grown with low (10 μM) and high (100 μM) Cd concentrations [12]. In the present study we further investigate tomato responses to 10 and 100 μM Cd concentrations at the root proteomic level, using 2-DE techniques. Roots were selected as the first tissue to explore since they are the first step in plant Cd assimilation, thus being the main site of toxic metal exposure, and also because previous results suggested that one of the Cd detoxification strategies in tomato plants relies on Cd allocation in roots [12]. Proteomic approaches have been taken elsewhere to study other stress related responses in tomato such as Fe deficiency in roots [40] and waterlogging in leaves [41], among others, and in general could provide a good overview of major metabolic changes occurring in response to stress.

2. Materials and methods

2.1. Plant culture

Tomato (*Lycopersicon esculentum* Mill cv. Tres Cantos) plants were grown in a controlled environment chamber, as indicated in [12]. Seeds were grown for two weeks in vermiculite, for two additional weeks in half-strength Hoagland nutrient solution and then transplanted to 10 L plastic buckets (18 plants per bucket) containing half-strength Hoagland nutrient solution with 45 μM Fe(III)-EDTA and 0, 10 or 100 μM $CdCl_2$, and grown in these conditions for ten more days. Whole roots were harvested, frozen in liquid N_2 and stored at −80 °C until further analysis. Five different batches of plants (5 biological replicates) were grown and analysed for proteomic profiling (Fig. S1).

2.2. Protein extraction

For protein extraction, roots of two plants from the same treatment in a given batch were pooled; approximately 1 g of root material was ground in liquid N_2 using a Retsch M301 mill (Retsch GmbH, Haan, Germany), and then homogenized in 5 mL of phenol, saturated with Tris-HCl 0.1 M (pH 8.0) containing 5 mM β-mercaptoethanol, by stirring for 30 min at 4 °C. After incubation, the homogenate was filtered (PVDF, 0.45 μm) and centrifuged at 5000×*g* for 15 min. The phenol phase was re-extracted for 30 min with one volume of phenol-saturated Tris-HCl 0.1 M (pH 8.0) containing 5 mM β-mercaptoethanol, and centrifuged as described above. The phenol phase was collected, and proteins precipitated by adding four volumes of 0.1 M ammonium acetate in cold methanol, using an incubation of at least 4 h at −20 °C. Samples were then centrifuged at 5000×*g* for 15 min and the pellet was washed three times with cold methanol, dried with N_2 gas and resuspended in sample rehydration buffer containing 8 M urea, 2% (w/v) CHAPS, 50 mM DTT, 2 mM PMSF and 0.2% (v/v) 3–10 ampholytes (Amersham, Uppsala, Sweden). After rehydration, samples were incubated at 38 °C for 2.5 h and then centrifuged at 15,000×*g* for 10 min at 20 °C. Protein concentration was measured with RC DC Protein Assay BioRad (BioRad, Hercules, CA, USA) based on the Lowry method. Samples were analysed by 2-DE immediately.

2.3. Protein 2-DE separation

Preliminary 2-DE experiments were carried out using a first dimension IEF separation with a linear pH gradient 3–10; in these conditions most of the spots were concentrated in the central region of the 2-DE gel (results not shown); therefore, to prevent protein co-migration and improve resolution a narrower pH gradient was chosen. A first dimension IEF separation [42] was carried out on 7 cm ReadyStrip IPG Strips

(BioRad) with a linear pH gradient pH 5–8 in a Protean IEF Cell (BioRad). Strips were rehydrated for 16 h at 20 °C in 125 μL of rehydration buffer containing 100 μg of root extract proteins and a trace of bromophenol blue, and then transferred onto a strip tray. IEF was run at 20 °C, for a total of 14,000 V h (20 min with a 0–250 V linear gradient, 2 h with a 250–4000 V linear gradient and 4000 V until 10,000 V h). After IEF, strips were equilibrated for 10 min in equilibration solution I (6 M urea, 0.375 M Tris-HCl, pH 8.8, 2% (w/v) SDS, 20% (v/v) glycerol, 2% (w/v) DTT) and for another 10 min in equilibration solution II (6 M urea, 0.375 M Tris-HCl pH 8.8, 2% (w/v) SDS, 20% (v/v) glycerol, 2.5% (w/v) iodoacetamide).

For the second dimension SDS PAGE, equilibrated IPG strips were placed on top of vertical 12% SDS-polyacrylamide gels (8×10×0.1 cm) and sealed with melted 0.5% agarose in 50 mM Tris-HCl, pH 6.8, containing 0.1% SDS. SDS PAGE was carried out at 20 mA per gel for approximately 1.5 h, until the bromophenol blue reached the plate bottom, in a buffer containing 25 mM Tris, 1.92 M glycine, and 0.1% SDS, at room temperature. Gels were subsequently stained with Coomassie-blue R-250 (Sigma, Barcelona, Spain). Gels were made from independent root preparations from five different batches of plants for each treatment.

2.4. Gel image and statistical analysis

Stained gels were scanned with a Bluescan48 Scanner (LaCie, Portland, OR, USA). Spot detection, gel matching and interclass analysis were performed with PDQuest 8.0 software (BioRad). The spots were also manually checked, and a high level of reproducibility between normalized spot volumes was found in the different replicates (Table S1).

Univariate and multivariate statistical analyses were carried out, using only spots present at least in 80% of gels in the same treatment. Differentially expressed spots were defined using a Student *t*-test ($p<0.10$). Partial Least Square (PLS) analysis was carried out using Statistica software (v. 9, Statsoft Inc. Tulsa, OK), either using all the spots or only those identified successfully by MS (see below).

2.5. In gel digestion and sample preparation for mass spectrometric analysis

Spots showing changes statistically significant (at $p<0.10$) and above a 2-fold threshold were excised automatically using a spot cutter (ProPic station from Genomic Solutions, Holliston, MA, USA, or EXQuest from BioRad) and then digested automatically using a ProGest protein digestion station (Genomic Solutions). The digestion protocol started with two de-staining steps, 30 min each, with 40% v/v acetonitrile (ACN) containing 200 mM NH_4HCO_3, followed by two washing steps, first with 25 mM NH_4HCO_3 for 5 min and then with 50% v/v ACN containing 25 mM NH_4HCO_3, for 15 min. After washing, gel spots were dehydrated with 100% ACN for 5 min, and then dried. Gel spots were rehydrated with 10 μL of a trypsin solution (12.5 ng μL^{-1} in 25 mM $(NH_4)_2CO_3$) for 10 min and then digested for 12 h at 37 °C. Digestion was stopped by adding 10 μL of TFA 0.5%. Peptides were purified automatically using a ProMS station (Genomic Solutions) with a C_{18} microcolumn (ZipTip, Millipore, MA, USA), and eluted directly onto a MALDI plate with 1 μL of matrix solution (5 mg mL^{-1} CHCA in 70% ACN/ 0.1% TFA v/v).

2.6. MALDI–TOF–MS, LIFT TOF–TOF analysis and identification of proteins

Peptide mass fingerprint spectra were determined on a 4700 Proteomics Analyzer (Applied Biosystems, Foster City, US) in positive ion reflector mode. Each spectrum was internally calibrated with *m/z* signals of porcine trypsin autolysis ions, and the typical mass measurement accuracy was ±20 ppm. Whenever possible, fragmentation spectra of the five most intense peaks were obtained for each sample. The measured tryptic peptide masses were searched in the NCBInr database 20070131, taxonomy Viridiplantae (283,672 sequences), using MASCOT software (Matrix Science, London, UK). When available, MS–MS data from LIFT TOF–TOF spectra were combined with MS peptide mass fingerprint data for database search. The following parameters were used for the database search: green plants taxonomic group, complete carbamidomethylation of cysteine residues, partial oxidation of methionine residues, mass tolerance of 100 ppm and one miscleavage allowed. MASCOT protein scores >76 were considered as significant ($p<0.05$). Protein scores are derived from ion scores as a non-probabilistic basis for ranking protein hits. Sequence coverage was always above 16% and at least 9 peptides were matched to the identified protein when peptide sequencing was not possible.

2.7. Metabolic pathway identification for proteins

We used the KOBAS software (http://kobas.cbi.pku.edu.cn) to assign the biochemical pathway for each protein identified by MS [40]. This software assigns a given set of proteins to known pathways in the KEGG database (http://www.genome.jp/kegg/pathway.html). All proteins in a common pathway were grouped manually. When no information was available in the KEGG database we searched for GO (http://www.geneontology.org/) annotation of the individual proteins.

3. Results and discussion

In a previous study we found that plant growth was reduced in both Cd treatments (10 and 100 μM Cd), and that leaves showed chlorosis symptoms when grown at 10 μM Cd and necrotic spots when grown at 100 μM Cd [12]. Root browning was observed in both treatments. Changes in plant mineral concentrations, including Cd, and in several metabolic activities related to C metabolism and in photosynthetic parameters were also found [12]. These previous results suggested that Cd detoxification strategies in tomato plants grown in the presence of Cd rely on root Cd accumulation, although at high Cd concentrations roots are overloaded with Cd and a significant mobilization to the shoots occurs.

3.1. Protein expression profiles and pathway analysis

Changes induced by Cd toxicity in the polypeptide pattern of root extracts from tomato plants grown at different Cd

concentrations (0, 10 and 100 μM Cd) were studied by 2-DE (IEF–SDS PAGE). Typical real scans of 2-DE gels obtained from root extracts from 0, 10 and 100 μM Cd supplied plants are shown in Fig. 1A, B and C, respectively. A total of 140 spots were consistently detected in gels of root extracts (spots present at least in 80% gels of one class or 50% of total gels). The average number of detected spots was (in mean ± SD) 121 ± 33, 145 ± 35 and 93 ± 38 in 0, 10 and 100 μM Cd 2-DE gels, respectively; approximately 87, 86 and 78% of spots were consistent in each class, respectively. To better describe changes in polypeptide composition we built a composite averaged virtual map containing all spots present in all 15 gels (5 per treatment; Fig. 1D, E and F).

The intensity of 43 and 45 spots changed significantly in the 10 and 100 μM Cd treatments, respectively, when compared to the control (Student *t*-test, $p < 0.10$). From these, 36 and 41 spots showed a relative intensity change above 2-fold in the 10 and 100 μM Cd treatments, respectively, when compared to the control. The PLS analysis showed a good separation between treatments when using all spots (Fig. 2A), and similar results were obtained when the analysis was carried out using only identified spots (Fig. 2B). The importance of the different spots in the PLS analysis is shown in Table S2; 19 out of the 25 most important spots were among those identified (Table 1).

The statistical analysis of averaged maps indicated that 10 μM Cd caused increases in signal intensity of 22 spots (orange symbols in Fig. 1E), whereas 6 spots were present in the 10 μM Cd treatment but absent in the control (red symbols in Fig. 1E). Among them, 21 spots matched reliably to known proteins in the NCBInr database (spots labeled 1–21 in Fig. 3A and Table 1), and their metabolic functions were assessed using KOBAS. Up-accumulated proteins belonged to different metabolic pathways including carbohydrate metabolism (spots 5, 12, 18, 19 and 21), cell wall organization (spots 2, 4, 8, 13 and 20), TCA cycle (spots 9 and 10), energy metabolism (spots 16 and 17), and protein metabolism, including protein folding (spots 1, 7, 11, 14 and 15) and peptidases (spots 3 and 6). A smaller group of spots showed decreases in relative intensity in plants grown at 10 μM Cd when compared to the controls. These included 7 spots with lower signal intensity (green symbols in Fig. 1E) and 1 spot not detected in Cd treated plants (blue symbol in Fig. 1E). Out of them, six were identified (spots labeled 22–27 in Fig. 3A and Table 1), and according to KOBAS assigned to glycolysis (spots 22, 24, 25 and 26), cell wall organization (spot 23) and TCA cycle (spot 27).

When comparing the averaged map of the 100 μM Cd treatment with that of control plants, 9 spots showed relative increases in signal intensity (orange symbols in Fig. 1F) and 2 more were detected *de novo* (red symbols in Fig. 1F). All of them were identified (spots labeled 28–36, and spots 8 and 18 in Fig. 3B and Table 1). Up-accumulated proteins in the 100 μM Cd treatment belonged to metabolic pathways including cell wall organization (spots 8, 28 and 36), glycolysis (spots 18 and 31)

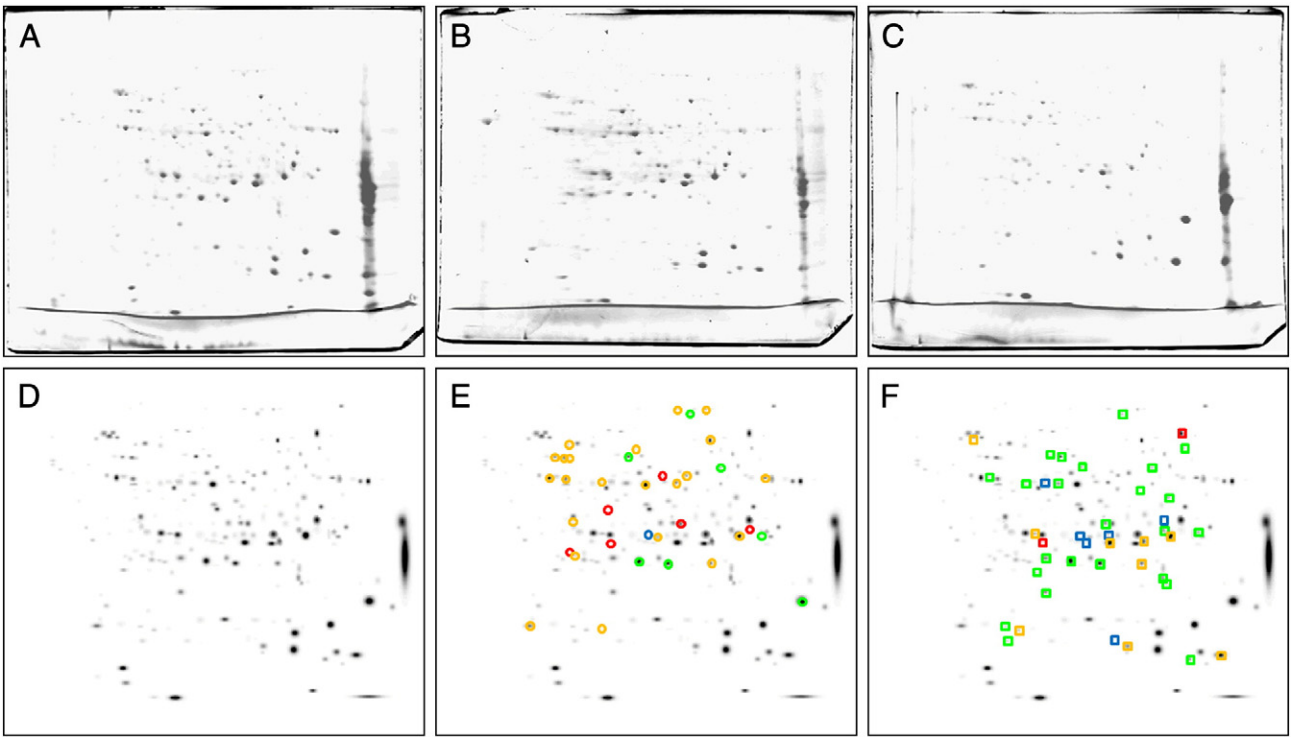

Fig. 1 – 2-DE IEF–SDS PAGE proteome maps of root extracts from 0, 10 and 100 μM $CdCl_2$ treated tomato plants. Proteins were separated in the first dimension in linear (pH 5–8) IPG gel strips and in the second dimension in 12% acrylamide vertical gels. Scans of typical gels of roots from 0, 10 and 100 μM Cd treated plants are shown in A, B and C, respectively. To facilitate visualization of the studied spots, a virtual composite image (D, E, and F) was created containing all spots present in the real gels A, B and C. In E (10 μM Cd) and F (100 μM Cd) spots whose intensities decreased or were no longer detected when compared to control maps were marked with green and blue symbols, respectively, and those with increased intensities or newly detected ones were marked with yellow and red symbols, respectively.

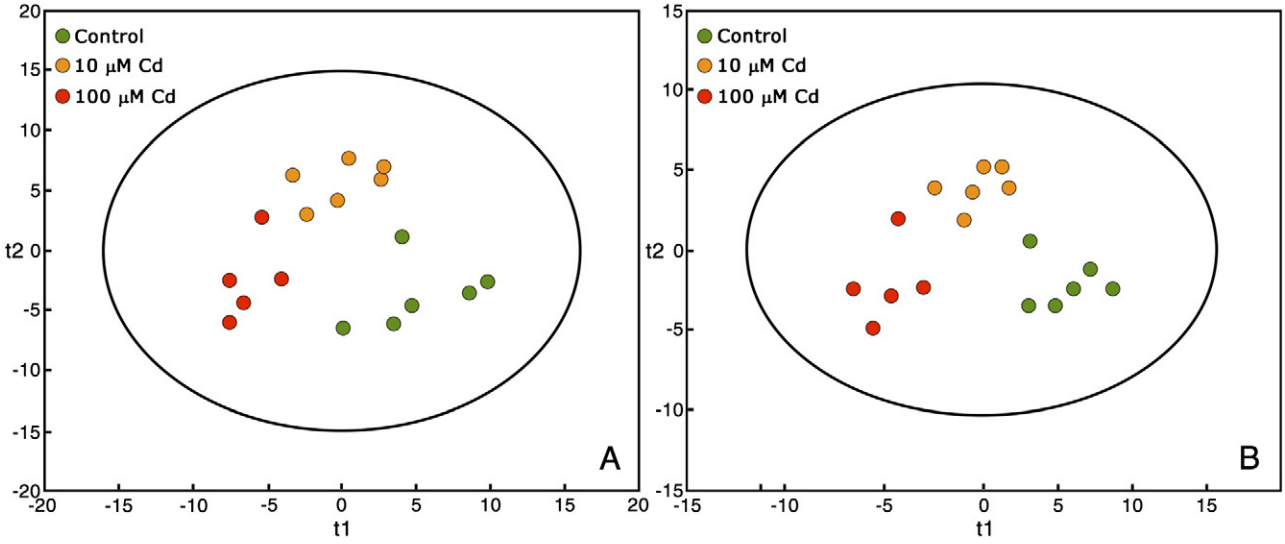

Fig. 2 – Multivariate statistical analysis (Partial Least Square, PLS) of 2-DE gels. Score scatter PLS plot of component 1 *vs.* component 2 after analysis of all (A) and identified spots (B) from roots of tomato plants grown in control 0 (green circles), 10 (orange circles) and 100 μM Cd (red circles). Only spots present in at least 80% of the gels in a given treatment were considered.

and TCA cycle (spots 32 and 33). Proteins involved in different stress related processes such as pathogenesis (spots 29 and 35), protein folding (spot 30), and glutathione metabolism (spot 34) showed also relative intensity increases. A large number of spots showed decreases in relative intensity in root extracts from plants grown at 100 μM Cd when compared to control plants. These included 24 spots with decreased intensity (green symbols in Fig. 1F) and 6 more not detected in 100 μM Cd treated plants (blue symbols in Fig. 1F). Among them, 22 spots were identified (Fig. 3B and Table 1) and according to KOBAS assigned to carbohydrate metabolism (spots 22, 24, 25, 26, 37, 38, 39, 41, 50, and 52), TCA cycle (spots 27 and 51), energy metabolism (spot 47 and 48), gene regulation (spots 40, 45 and 46), cell wall organization (spots 42 and 44), oxidative stress protection (spot 49), N metabolism (spot 53), and ascorbate metabolism (spot 43).

To summarize, between 93 and 145 spots were detected in gels from root extracts and approximately 25% and 44% of these spots showed significant changes in relative intensities as a result of exposure to 10 and 100 μM Cd, respectively (Table S3). The total number of spots detected was relatively low when compared to other proteomic studies in tomato roots [40,43]. Several causes may account for this discrepancy, including i) protein extraction method and amount of protein loaded in the gels, ii) gel size, iii) pI range and iv) sensitivity of the staining method. Proteomic results described to date have shown changes in relative intensity in 5–20% of spots in response to Cd toxicity in different plant species and tissues [30–34].

3.2. *Effect of Cd toxicity on metabolic pathways*

3.2.1. *Primary carbon metabolism*

3.2.1.1. *Carbohydrate metabolism and glycolysis*. Five spots corresponding to three proteins of the glycolytic pathway, pyruvate dehydrogenase (PDH), glyceraldehyde 3-phosphate dehydrogenase (GADPH) and enolase (3 spots) increased in relative amount in roots grown with 10 μM Cd when compared to the controls (Table 1). GADPH (spot 18) and two spots identified as enolase (spots 5 and 12) increased 2-, 3- and 4-fold, respectively, while PDH (spot 21) and one spot identified as enolase (spot 19) were newly detected in the 10 μM Cd treatment when compared to the controls. In the 100 μM Cd treatment, PDH (spot 31) and GADPH (spot 18) also increased, although only 2-fold. On the other hand, Cd exposure caused decreases in intensity in 3 and 7 proteins involved in carbohydrate metabolism in the low and high Cd treatments, respectively. In the 10 μM Cd treatment, decreases (expressed as % of control values) of 60, 50, 60 and 70% were measured for fructokinase (spots 22 and 26), dihydrolipoamide dehydrogenase (spot 25) and phosphoglycerate mutase (PGM) (spot 24), respectively. In the 100 μM Cd treatment, large decreases in intensity were measured for enolase (60% for spot 37; spot 50 was lost), GADPH (spot 39, 70%; spot 52 was lost), phosphoglycerate kinase (spot 38, 70%), triosephosphate isomerase (spot 41, 60%), PGM (spot 24, 60%), dihydrolipoamide dehydrogenase (spot 25, 80%) and fructokinase (spots 22 and 26, 70% each).

Overall, our results show that an up-regulation of the glycolytic pathway occurs at 10 μM Cd, whereas at 100 μM Cd a general down-regulation of the carbohydrate metabolism takes place. Reports in the literature regarding Cd-induced changes in carbohydrate metabolism proteins have been contradictory. Decreases in several proteins (enolase, GADPH, fructokinase and PGM) have been described in roots of two Cd-tolerant plants, poplar and *B. juncea*, after exposure to 20 and 250 μM Cd, respectively, whereas in the model plant *A. thaliana* grown with 10 μM Cd and in *A. thaliana* cell cultures increases in GADPH and other glycolytic enzymes were measured [28,34,35,44]. These reports, together with those in the present study, indicate that changes in carbohydrate metabolism upon Cd exposure are dose and species dependent.

Several changes were common to both levels of Cd toxicity including the increase in PDH and the decreases in fructokinase,

Table 1 – Proteins identified in 2-DE IEF–SDS PAGE gels. MS[1] Protein score is –10*Log (P), where P is the probability that the observed match is a random event. Protein scores >76 were considered significant ($p<0.05$). – indicates no changes in relative abundance.

No.	Teor. MW/pI	Exp. MW/pI	*vs.* 10 Cd/ *vs.* 100 Cd	Cov.	Score/pep/ion	ID	Homology	Species	Matched pathway in KEGG
1	62/5.2	67/5.8	+3.0/–	44	240/20/3	gi|300265	HSP68 heat stress DNAK homolog	*Solanum perivarum*	Chaperones and folding catalysts; pores ion channels; MAPK signaling pathway
2	38/5.3	43/5.9	+5.6/–	31	139/11/2	gi|3219772	Actin-51	*Solanum lycopersicum*	Cytoskeleton proteins
3	27/5.6	28/6.1	+2.2/–	75	328/15/3	gi|77999303	Proteasome-like protein alpha subunit	*Solanum tuberosum*	Peptidases; proteasome
4	42/5.8	40/6.6	+4.5/–	56	459/23/4	gi|48478827	UDP-glucose:protein transglucosylase-like protein Sl-UPTG1	*Lycopersicon esculentum*	
5	48/5.7	50/6.4	+3.0/–	63	890/22/5	gi|119354	Enolase 2-phosphoglycerate-dehydratase	*Solanum lycopersicum*	Glycolysis/gluconeogenesis
6	61/7.9	52/6.8	+2.5/–	41	276/21/3	gi|27463709	Neutral leucine aminopeptidase preprotein	*Solanum lycopersicum*	Peptidases
7	65/5.8	70/7.0	+2.4/–	17	83/7/2	gi|28973653	Putative TPR-repeat protein	*Arabidopsis thaliana*	Chaperones and folding catalysts
8	38/6.6	35/7.0	+2.7/+28.9	56	481/19/4	gi|461978	Glucan endo 1–3 beta glucosidase A	*Solanum lycopersicum*	Starch and sucrose metabolism
9	98/5.8	96/7.0	+3.0/–	46	535/32/4	gi|30407706	Aconitase	*Solanum pennellii*	Citrate cycle (TCA cycle); reductive carboxylate cycle (CO2 fixation); glyoxylate and dicarboxylate metabolism
10	70/5.9	64/6.4	+5.0/–	31	210/16/2	gi|15240075	SDH1-1	*Arabidopsis thaliana*	Citrate cycle (TCA cycle); oxidative phosphorylation
11	63/5.7	59/5.8	+11.6/–	37	332/18/5	gi|1762130	Chaperonin 60 beta subunit	*Solanum tuberosum*	Chaperones and folding catalysts
12	48/5.7	51/6.1	+4.5/–	64	735/24/5	gi|119354	Enolase 2-phosphoglycerate-dehydratase	*Solanum lycopersicum*	Glycolysis/gluconeogenesis
13	52/5.7	51/6.7	+4.4/–	50	576/35/4	gi|136739	UTP-glucose-1-phosphate uridylyltransferase (UDP-glucose pyrophosphorylase)	*Solanum tuberosum*	Pentose and glucuronate interconversions; nucleotide sugars metabolism; galactose metabolism
14	63/5.7	59/5.7	+2.3/–	37	310/19/4	gi|1762130	Chaperonin-60 beta subunit	*Solanum tuberosum*	Chaperones and folding catalysts
15	58/5.3	59/5.8	+2.3/–	36	226/16/2	gi|24637539	Heat shock protein 60	*Prunus dulcis*	Chaperones and folding catalysts
16	60/5.9	51/5.7	+2.4/–	53	758/22/5	gi|114421	ATP synthase subunit beta, mitochondrial precursor	*Nicotiana plumbaginifolia*	Oxidative phosphorylation
17	60/5.9	51/5.8	+2.4/–	53	758/22/5	gi|114421	ATP synthase subunit beta, mitochondrial precursor	*Nicotiana plumbaginifolia*	Oxidative phosphorylation
18	37/6.3	40/7.2	+2.4/+2.7	61	526/19/4	gi|22094849	Glyceraldehyde 3-phosphate dehydrogenase	*Solanum tuberosum*	Glycolysis/gluconeogenesis
19	48/5.7	52/6.6	New/–	68	751/24/5	gi|119354	Enolase 2-phosphoglycerate-dehydratase	*Solanum lycopersicum*	Glycolysis/gluconeogenesis
20	39/5.9	43/6.8	New/–	43	523/15/4	gi|7430935	Probable cinnamyl–alcohol dehydrogenase (EC1.1.1.195)	*Solanum lycopersicum*	Other enzymes
21	44/8.1	41/7.3	New/–	54	423/22/4	gi|12003246	Pyruvate dehydrogenase	*Solanum lycopersicum*	Glycolysis/gluconeogenesis; butanoate metabolism; valine, leucine and isoleucine biosynthesis; alanine and aspartate metabolism; pyruvate metabolism
22	35/5.8	35/6.4	–2.6/–3.4	81	853/29/5	gi|75221385	Fructokinase-2	*Solanum lycopersicum*	Fructose and mannose metabolism; starch and sucrose metabolism

(continued on next page)

Table 1 *(continued)*

No.	Teor. MW/pI	Exp. MW/pI	*vs.* 10 Cd/ *vs.* 100 Cd	Cov.	Score/pep/ion	ID	Homology	Species	Matched pathway in KEGG
23	35/6.2	31/7.7	−2.9/–	53	521/11/5	gi|544011	Basic 30 kDa endochitinase precursor	*Solanum lycopersicum*	Aminosugars metabolism
24	61/5.4	59/6.3	−2.1/−2.8	41	426/16/2	gi|4582924	Phosphoglycerate mutase	*Solanum tuberosum*	Glycolysis/gluconeogenesis
25	53/6.9	53/7.1	−2.3/−6.0	38	146/13/1	gi|23321340	Dihydrolipoamide dehydrogenase precursor	*Solanum lycopersicum*	Citrate cycle (TCA cycle); pyruvate metabolism; glycolysis/gluconeogenesis; valine, leucine and isoleucine degradation; alanine and aspartate metabolism; glycine, serine and threonine metabolism
26	35/5.8	35/6.6	−2.0/−2.7	47	101/13/0	gi|75221385	Fructokinase-2	*Solanum lycopersicum*	Fructose and mannose metabolism; starch and sucrose metabolism
27	36/5.7	40/6.5	Lost/Lost	58	187/15/2	gi|83283965	Malate dehydrogenase-like protein	*Solanum tuberosum*	Citrate cycle (TCA cycle); pyruvate metabolism; reductive carboxylate cycle (CO2 fixation); glyoxylate and dicarboxylate metabolism; carbon fixation
28	28/5.9	28/6.0	–/+4.0	69	323/12/4	gi|544007	Acidic 26 kDa endochitinase precursor	*Solanum lycopersicum*	Aminosugars metabolism
29	28/5.8	23/7.6	–/+2.8	45	402/6/4	gi|31095603	PR5-like protein	*Solanum lycopersicum*	
30	73/5.1	73/5.6	–/+2.1	43	611/29/4	gi|1346172	Luminal-binding protein precursor (BiP) (78 kDa glucose-regulated protein homolog)	*Solanum lycopersicum*	MAPK signaling pathway; pores ion channels; chaperones and folding catalysts
31	40/5.5	40/6.1	–/+2.4	17	148/6/2	gi|3851003	Pyruvate dehydrogenase E1 beta subunit isoform 3	*Zea mays*	Pyruvate metabolism; glycolysis/ gluconeogenesis; butanoate metabolism; valine, leucine and isoleucine biosynthesis; alanine and aspartate metabolism
32	36/6.1	39/6.7	–/+2.1	70	451/17/3	gi|77999077	Malate dehydrogenase	*Lycopersicon chilense*	Pyruvate metabolism; reductive carboxylate cycle (CO2 fixation); glyoxylate and dicarboxylate metabolism; citrate cycle (TCA cycle); carbon fixation
33	36/8.8	39/7.0	–/+2.2	46	106/9/1	gi|52139816	Mitochondrial malate dehydrogenase	*Lycopersicon esculentum*	Pyruvate metabolism; reductive carboxylate cycle (CO2 fixation); glyoxylate and dicarboxylate metabolism; citrate cycle (TCA cycle); carbon fixation
34	24/5.8	24/6.9	–/+2.4	39	195/7/4	gi|2290782	Glutathione S-transferase, class phi	*Solanum commersonii*	MAPK signaling pathway; metabolism of xenobiotics by cytochrome P450; glutathione metabolism
35	38/6.7	75/7.3	–/New	13	118/7/1	gi|2230959	Pathogenesis related protein P69G	*Lycopersicon esculentum*	

36	42/5.8	38/6.2	–/New	45	135/14/1	gi|48478827	UDP-glucose:protein transglucosylase-like protein SlUPTG1	*Lycopersicon esculentum*	
37	48/5.7	51/6.3	–/–2.5	63	417/20/4	gi|119354	Enolase (2-phosphoglycerate-dehydratase)	*Solanum lycopersicum*	Glycolysis/gluconeogenesis
38	42/6.0	43/6.7	–/–3.5	38	285/12/3	gi|82621108	Phosphoglycerate kinase-like	*Solanum tuberosum*	Glycolysis/gluconeogenesis Carbon fixation
39	32/5.9	41/7.2	–/–3.6	19	111/4/1	gi|2078298	Glyceraldehyde 3-phosphate dehydrogenase	*Lycopersicon esculentum*	Glycolysis/gluconeogenesis
40	99/8.1	34/6.1	–/–3.0	21	82/16/0	gi|108710078	Transposon protein, putative, CACTA, En/Spm sub-class	*Oryza sativa*	
41	28/5.5	28/5.9	–/–2.5	17	279/4/3	gi|1351282	Triosephosphate isomerase, cytosolic	*Stellaria longipes*	Glycolysis/gluconeogenesis; carbon fixation; fructose and mannose metabolism; inositol metabolism
42	70/8.0	65/7.4	–/–13.6	39	507/23/4	gi|37359708	LEXYL2	*Solanum lycopersicum*	Starch and sucrose metabolism; cyanoamino acid metabolism; phenylpropanoid biosynthesis
43	43/8.9	49/7.0	–/–29.9	49	269/18/3	gi|72011375	Monodehydroascorbate reductase	*Lycopersicon esculentum*	Ascorbate and aldarate metabolism
44	39/6.7	41/7.5	–/–2.3	21	311/9/3	gi|13591616	UDP-D-glucuronate carboxy-lyase	*Pisum sativum*	Polyketide sugar unit biosynthesis; biosynthesis of vancomycin group antibiotics; streptomycin biosynthesis; nucleotide sugars metabolism
45	29/7.0	32/6.2	–/–2.2	25	76/5/1	gi|82621186	Transcription factor APFI-like	*Solanum tuberosum*	
46	22/9.6	33/7.2	–/–12.7	45	77/9/0	gi|110681480	Putative transcription factor	*Platanus x acerifolia*	
47	60/6.3	53/6.5	–/–2.1	50	447/22/4	gi|410633	Cytochrome c reductase-processing peptidase subunit I, MPP subunit I,	*Solanum tuberosum*	Peptidases
48	60/5.9	52/5.7	–/–2.9	56	706/23/5	gi|114421	ATP synthase subunit beta, mitochondrial precursor	*Nicotiana plumbaginifolia*	Oxidative phosphorylation
49	22/6.0	22/7.4	–/–2.3	26	221/5/2	gi|15239652	FQR1 (flavodoxin-like quinone reductase 1)	*Arabidopsis thaliana*	General function prediction only
50	48/5.7	51/6.2	–/Lost	63	624/21/5	gi|119354	Enolase (2-phosphoglycerate-dehydratase)	*Solanum lycopersicum*	Glycolysis/gluconeogenesis
51	36/8.9	38/6.5	–/Lost	55	193/11/2	gi|52139816	Mitochondrial malate dehydrogenase	*Solanum chilense*	Carbon fixation; citrate cycle (TCA cycle); pyruvate metabolism; reductive carboxylate cycle (CO2 fixation); glyoxylate and dicarboxylate metabolism
52	32/5.9	40/6.7	–/Lost	45	342/11/4	gi|2078298	Glyceraldehyde 3-phosphate dehydrogenase	*Lycopersicon esculentum*	Glycolysis/gluconeogenesis
53	45/6.3	44/7.2	–/Lost	52	420/20/4	gi|71834851	NADH-glutamate dehydrogenase	*Lycopersicon esculentum*	D-glutamine and D-glutamate metabolism; arginine and proline metabolism; nitrogen metabolism; glutamate metabolism

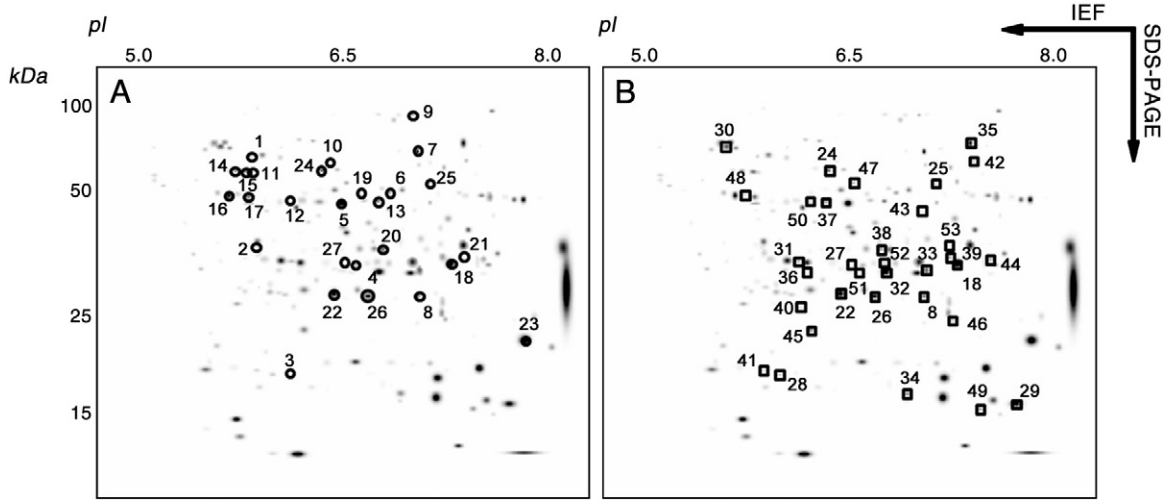

Fig. 3 – Polypeptides identified in root extracts of plants grown with 10 (circles in A) and 100 μM Cd (squares in B). Polypeptides with significant homologies to proteins present in databases (using MALDI MS–MS and MASCOT, described in detail in Table 1) were annotated on a virtual composite gel image (see Fig. 1).

PGM and dihydrolipoamide dehydrogenase, which may constitute a general response to Cd toxicity in tomato. The decrease in the relative amount of fructokinase in Cd toxicity indicates that glucose is preferred over fructose as initial substrate in the glycolytic pathway, and this could be related to the use of starch as an energy source instead of sucrose. This hypothesis would be in consonance with the low photosynthetic rates measured in these plants [12] that would cause a shortage of available sucrose.

Interestingly, changes in the glycolytic pathway observed in the 10 μM Cd treatment have been described at the proteomic level in roots of Fe-starved tomato plants [40]. Moreover, a Cd-induced Fe deficiency has been described before at the physiological level [11,12,45]; also, the Fe concentration in leaves of tomato plants grown at low Cd concentrations were 50% lower than that measured in control plants while in plants grown at 100 μM Cd leaf Fe concentrations did not change [12]. Therefore, we propose that the toxicity changes observed at low Cd are likely due to a Cd-induced Fe deficiency; conversely, changes found when plants are exposed to high Cd would reflect a shutdown of carbohydrate metabolism as result of true Cd toxicity.

3.2.1.2. *TCA cycle*. Aconitase (spot 9) and succinate dehydrogenase (spot 10) increased 3- and 5-fold in the 10 μM Cd treatment when compared to control plants, suggesting an up-regulation of the TCA cycle; however, at 100 μM Cd no changes in these proteins were found. Concerning malate dehydrogenase (MDH), four different spots were identified. One of them was no longer detected at 10 μM Cd (spot 27), whereas at 100 μM Cd the two more abundant spots were up-regulated (spots 32 and 33, approximately 2-fold) and the two less abundant spots disappeared (spots 27 and 51) (Table S1). Increases in root activities of several TCA cycle enzymes, including MDH, have been described in tomato plants grown with 10 and 100 μM Cd [12]. Also, in *Arabidopsis* roots and *Arabidopsis* cell cultures increases in proteins involved in the TCA cycle have been measured after Cd exposure [28,34]. In contrast, the relative amount of a large number of TCA-related proteins decreased in poplar roots exposed to a Cd excess [44]. These facts are in line with changes observed in glycolysis, and may point to differences between Cd-tolerant and Cd-sensitive species. Also, increases in TCA-related proteins and activities have been described in roots of Fe-deficient plants [40,46], which again supports that low Cd exposure may elicit a response similar to that of Fe deficiency. Differences in the MDH polypeptidic pattern in Cd exposed tomato roots may be due to the existence of different isoforms, possibly with different intracellular localization (cytosolic and mitochondrial) and functions (TCA and non-TCA-related), and/or the presence of PTMs.

3.2.2. *Energy metabolism*

Low Cd treatment (10 μM) caused an increase in the relative amount of the ATP synthase subunit beta, represented by 2 spots (spots 16 and 17; 2-fold increases over control values). However, at high Cd supply, energy production seemed to be down-regulated, since the ATP synthase subunit beta (spot 48), and cytochrome c reductase-processing peptidase subunit I (spot 47) decreased markedly (by 70 and 50%, respectively) when compared to the controls. Again, results suggest that low Cd concentrations elicit responses similar to those observed in Fe-deficient roots, where respiratory activities increase [40,46]. Interestingly, no changes in ATP synthase were measured in Cd treated poplar [44]. The decrease in energy production at 100 μM Cd might be related not only to the decreased glycolysis and TCA activities, but to other effects of Cd toxicity, as suggested by the decrease in the relative amount of a proccessing peptidase responsible for cytochrome c reductase synthesis.

3.2.3. *Cell wall and cytoskeleton*

Root Cd exposure caused a reorganization of cell wall composition at both Cd concentrations, as revealed by several protein changes. Ten micromolar induced relative increases in three proteins related to cell wall organization, Sl-UPTG1,

glucan endo 1–3 betaglucosidase A and UTP-glucose-1-phosphate uridyltransferase (spots 4, 8 and 13; 5-, 3- and 4-fold, respectively). Also, cinnamyl–alcohol dehydrogenase (spot 20) was detected *de novo*, and a 6-fold increase in a cytoskeleton protein, actin-51 (spot 2), was observed at 10 μM Cd. In the 100 μM Cd treatment, three of such proteins, Sl-UPTG1 (spot 36), glucan endo 1–3 betaglucosidase (spot 8) and acidic 26 kDa endochitinase precursor (spot 28) increased markedly (newly appearing, 29- and 4-fold, respectively). On the other hand, several proteins related to cell wall organization were down-regulated with Cd toxicity; this included a 70% decrease in a basic 30 kDa endochitinase precursor (spot 23) at 10 μM Cd and 93 and 50% decreases of LEXYL2 (spot 42) and UDP-D-glucuronate carboxy-lyase (spot 44) at 100 μM Cd.

Cell walls participate in metal binding and can play an important role in metal tolerance and accumulation. Cell wall reorganization has been described previously in heavy metal toxicities, including Cd [47]. In particular, an increase in cynnamyl alcohol deshydrogenase has been described previously in roots grown at Cu and Cd toxic concentrations [48]. Cell wall related changes observed in both Cd treatments were different to those observed in Fe-deficient tomato roots; for instance, decreases in glucan endo 1–3 betaglucosidase occur with Fe deficiency [40]. This suggests that changes found are not related specifically to Fe deficiency but instead may reflect generic heavy metal or stress responses, as also suggested by changes in several chitinases.

3.2.4. *Protein metabolism: protein folding and proteolysis*

Seven proteins related to protein metabolism were up-regulated in the 10 μM Cd treatment, whereas just one increased with 100 μM Cd. In the 10 μM Cd treatment there were relative increases in five chaperones: heat shock protein (HSP) 68 (spot 1; 3-fold), putative TPR-repeat protein (spot 7; 2-fold), chaperonin 60 beta subunit (spots 11 and 14; 12- and 2-fold) and HSP 60 (spot 15; 2-fold) and two peptidases: proteasome-like protein alpha subunit (spot 3; 2-fold) and neutral leucine aminopeptidase preprotein (spot 6; 3-fold). The 100 μM Cd treatment caused a 2-fold increase in a luminal-binding protein precursor (spot 30). Increases in chaperonin as well as in peptidase relative amounts have been described previously as a result of heavy metal toxicity and are a common marker of plant stress [44]. Chaperonins could prevent protein denaturation even in the presence of Cd in the cytoplasm, while proteases could recycle proteins unfolded by Cd. Interestingly, a larger number of these proteins was increased in the 10 μM when compared to the 100 μM Cd treatment, suggesting that in the high Cd treatment the plant has ceased to try to overcome Cd toxicity.

3.2.5. *Others*

The 100 μM Cd treatment caused increases in two plant stress related proteins, the PR5-like protein (spot 29; 3-fold) and the pathogenesis related protein P69G (spot 35; newly appearing), and also in gluthatione S-transferase class phi (GST; spot 34; 2-fold), a protein involved in gluthatione metabolism. Increases in GST, an enzyme that conjugates GSH to cytotoxic products, have been found in all root and cell culture proteomic studies on Cd toxicity to date, suggesting that this is a general plant response to Cd toxicity. On the other hand, PC synthesis has been widely described as a mechanism of Cd detoxification [19]. However, no components of S assimilation, cysteine or GSH biosynthesis were detected to change in response to Cd exposure in the present work, and just a couple of proteins related to S assimilation have been described to increase in other proteomic studies [34,35,44]. The absence of PCs in our gels may be due to the low MWs of these peptides, but also to experimental limitations as commented above (Section 3.1).

A 97% and a 60% decrease in monodehydroascorbate reductase (spot 43; MDAR) and flavin mononucleotide-binding flavodoxin-like quinone reductase (spot 49; FQR1), oxidative stress protecting enzymes [49], were measured at 100 μM Cd, and this might be associated with the increase in GST [44]. A decrease in MDAR has been also found with Cd treatment in poplar roots [44], although the opposite occurs in *B. juncea* roots [35]. Interestingly, MDAR changes were not observed in tomato roots grown at 10 μM Cd. High Cd treatment caused the disappeareance of glutamate dehydrogenase (GDH, spot 53), an enzyme involved in N metabolism. A similar decrease was measured in poplar roots [44] whereas in *A. thaliana* cell cultures an increase in this enzyme was found [28]. A general decrease in N assimilation in roots of Cd exposed plants has been described [44,50]. In a previous study with Cd treated tomato roots [50], protein concentration and transcript abundance of GDH did not change with Cd toxicity whereas GDH activity increased, suggesting the existence of allosteric regulation. Since GDH was the only enzyme related to N metabolism that changed with Cd toxicity, no conclusions can be drawn from our results regarding N metabolism.

Three proteins involved in gene regulation, the transposon protein CACTA (spot 40), the transcription factor APFI-like (spot 45) and the putative transcription factor (spot 46), decreased in the 100 μM Cd treatment (by 70, 50, and 92%, respectively).

4. Conclusion

An overview of the results is presented in Fig. 4. Our data suggest that different responses of the primary C metabolism occur in low *vs.* high Cd exposures. Low Cd toxicity (10 μM Cd) causes an up-regulation of the glycolytic pathway, TCA cycle and respiration, likely to produce energy to cope with the low photosynthetic rates of these plants [12]. These root responses, along with the leaf chlorophyll and Fe decreases [12], are similar to those observed in Fe-deficient plants, suggesting that at least some of the low Cd tomato responses are due to Fe deficiency, as also suggested by physiological studies [11,12,40,45]. At high Cd concentrations (100 μM) major decreases in growth [12], a shutdown of the carbohydrate metabolism and decreases in respiration occur, with no consistent changes in TCA cycle-related proteins (Fig. 4). Also, evidence for an increase in detoxifying activities (GST) was found. This suggests that effects are mainly linked to true Cd toxicity, perhaps associated to protein degradation by oxidative stress.

Also, these results, along with those of other proteomic and physiological studies, indicate that different responses of the primary C metabolism at low Cd concentrations are observed in tolerant *vs.* non tolerant plants. In non tolerant plants, such

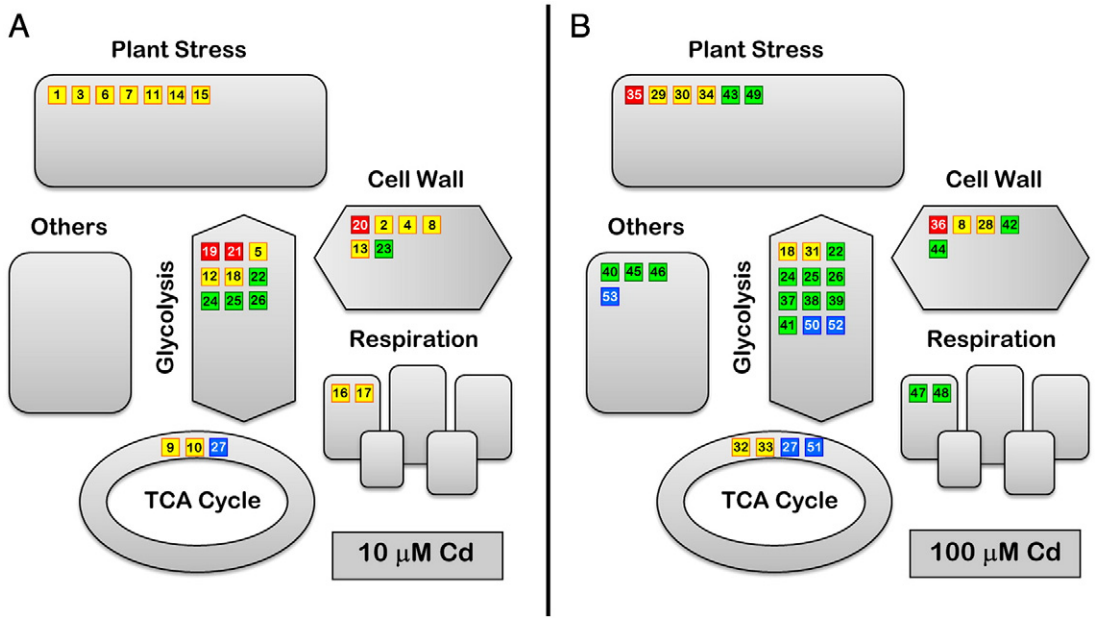

Fig. 4 – Changes in metabolic pathways as affected by Cd. Panels A and B are for 10 and 100 μM Cd treated plants, respectively. Pathways related to the identified proteins were integrated according to the KEGG database. A statistical Student *t*-test was performed to show relevant changes between samples. Red symbols mean newly detected proteins in Cd treated roots and yellow symbols proteins showing increases in intensity compared to control (using a 2-fold threshold change). The same threshold (decreases larger than 50%) was selected for proteins showing decreases in intensity (green symbols). Blue symbols indicate proteins not detected in Cd treated roots. Numbers correspond to those in Table 1.

as tomato, C and energy metabolism increase, whereas in tolerant plants, such as poplar, C metabolism decreased and energy metabolism did not change [30].

Acknowledgements

JRC and RRA were supported by I3P and FPI predoctoral fellowships from the CSIC and MCINN (Spanish Ministry of Science and Innovation), respectively. This work was supported by the MICINN (project AGL2007-61948, cofinanced with FEDER) and the Aragón Government (group A03). The authors thank Adelina Calviño for her help in growing and harvesting the plants.

Appendix A. Supplementary data

Supplementary data associated with this article can be found, in the online version, at doi:10.1016/j.jprot.2010.05.001.

REFERENCES

[1] Alloway BJ, Jackson AP, Morgan H. The accumulation of cadmium by vegetables grown on soils contaminated from a variety of sources. Sci Total Environ 1990;91:223–36.
[2] Adams ML, Zhao FJ, McGrath SP, Nicholson FA, Chambers BJ. Predicting cadmium concentrations in wheat and barley grain using soil properties. J Environ Qual 2004;33:532–41.
[3] Iribar V, Izco F, Tames P, Antigüedad I, da Silva A. Water contamination and remedial measures at the Troya abandoned Pb–Zn mine (The Basque Country, Northern Spain). Environ Geol 2000;39:800–6.
[4] Pinot F, Kreps SE, Bachelet M, Hainaut P, Bakonyi M, Polla BS. Cadmium in the environment: sources, mechanisms of biotoxicity, and biomarkers. Rev Environ Health 2000;15:299–323.
[5] Chen W, Chang AC, Wu L. Assessing long-term environmental risks of trace elements in phosphate fertilizers. Ecotoxicol Environ Saf 2007;67:48–58.
[6] Hardiman RT, Jacoby B. Absorption and translocation of Cd in bush beans *Phaseolus vulgaris*. Physiol Plant 1984;61:670–4.
[7] Korshunova YO, Eide D, Clark WG, Guerinot ML, Pakrasi HB. The IRT1 protein from *Arabidopsis thaliana* is a metal transporter with a broad substrate range. Plant Mol Biol 1999;40:37–44.
[8] Thomine S, Wang R, Ward JM, Crawford NM, Schroeder JI. Cadmium and iron transport by members of a plant metal transporter family in *Arabidopsis* with homology to Nramp genes. Proc Natl Acad Sci U S A 2000;97:4991–6.
[9] Perfus-Barbeoch L, Leonhardt N, Vavasseur A, Forestier C. Heavy metal toxicity: cadmium permeates through calcium channels and disturbs the plant water status. Plant J 2002;32:539–48.
[10] Senden MHMN, Wolterbeek HT. Effect of citric acid on the transport of cadmium through xylem vessels of excised tomato stem-leaf systems. Acta Bot Neerl 1990;39:297–303.
[11] Larbi A, Morales F, Abadía A, Gogorcena Y, Lucena JJ, Abadía J. Effects of Cd and Pb in sugar beet plants grown in nutrient solution: induced Fe deficiency and growth inhibition. Funct Plant Biol 2002;29:1453–64.
[12] López-Millán A-F, Sagardoy R, Solanas M, Abadía A, Abadía J. Cadmium toxicity in tomato (*Lycopersicon esculentum*) plants grown in hydroponics. Environ Exp Bot 2009;65:376–85.

[13] Ciscato M, Vangronsveld J, Valcke R. Effects of heavy metals on the fast chlorophyll fluorescence induction kinetics of photosystem II: a comparative study. J Biosci 1999;54:735–9.
[14] Dong J, Wu F, Zhang G. Influence of cadmium on antioxidant capacity and four microelement concentrations in tomato seedlings (*Lycopersicon esculentum*). Chemosphere 2006;64: 1659–66.
[15] Cuypers A, Vangronsveld J, Clijsters H. The chemical behaviour of heavy metals plays a prominent role in the induction of oxidative stress. Free Radic Res 1999;31:S39–43 Suppl.
[16] Chen YX, He YF, Luo YM, Yu YL, Lin Q, Wong MH. Physiological mechanism of plant roots exposed to cadmium. Chemosphere 2003;50:789–93.
[17] Lin R, Wang X, Luo Y, Du W, Guo H, Yin D. Effects of soil cadmium on growth, oxidative stress and antioxidant system in wheat seedlings (*Triticum aestivum* L.). Chemosphere 2007;69:89–98.
[18] Cobbett C, Goldsbrough P. Phytochelatins and metallothioneins: roles in heavy metal detoxification and homeostasis. Annu Rev Plant Biol 2002;53:159–82.
[19] Cobbett CS. Phytochelatins and their roles in heavy metal detoxification. Plant Physiol 2000;123:825–32.
[20] Lombi E, Tearall KL, Howarth JR, Zhao FJ, Hawkesford MJ, McGrath SP. Influence of iron status on cadmium and zinc uptake by different ecotypes of the hyperaccumulator *Thlaspi caerulescens*. Plant Physiol 2002;128:1359–67.
[21] Zhao FJ, Jiang RF, Dunham SJ, McGrath SP. Cadmium uptake, translocation and tolerance in the hyperaccumulator *Arabidopsis halleri*. New Phytol 2006;172:646–54.
[22] Kupper H, Mijovilovich A, Meyer-Klaucke W, Kroneck PM. Tissue- and age-dependent differences in the complexation of cadmium and zinc in the cadmium/zinc hyperaccumulator *Thlaspi caerulescens* (Ganges ecotype) revealed by X-ray absorption spectroscopy. Plant Physiol 2004;134:748–57.
[23] Weber M, Harada E, Vess C, Roepenack-Lahaye E, Clemens S. Comparative microarray analysis of *Arabidopsis thaliana* and *Arabidopsis halleri* roots identifies nicotianamine synthase, a ZIP transporter and other genes as potential metal hyperaccumulation factors. Plant J 2004;37:269–81.
[24] Ueno D, Ma JF, Iwashita T, Zhao FJ, McGrath SP. Identification of the form of Cd in the leaves of a superior Cd-accumulating ecotype of *Thlaspi caerulescens* using 113Cd-NMR. Planta 2005;221:928–36.
[25] Hernández-Allica J, Garbisu C, Becerril JM, Barrutia O, García-Plaizaola JI, Zhao FJ, et al. Synthesis of low molecular weight thiols in response to Cd exposure in *Thlaspi caerulescens*. Plant Cell Environ 2006;29:1422–9.
[26] Ma JF, Ueno D, Zhao FJ, McGrath SP. Subcellular localisation of Cd and Zn in the leaves of a Cd-hyperaccumulating ecotype of *Thlaspi caerulescens*. Planta 2005;220:731–6.
[27] Sobkowiak R, Deckert J. Proteins induced by cadmium in soybean cells. J Plant Physiol 2006;163:1203–6.
[28] Sarry JE, Kuhn L, Ducruix C, Lafaye A, Junot C, Hugouvieux V, et al. The early responses of *Arabidopsis thaliana* cells to cadmium exposure explored by protein and metabolite profiling analyses. Proteomics 2006;6:2180–98.
[29] Schneider T, Schellenberg M, Meyer S, Keller F, Gehrig P, Riedel K, et al. Quantitative detection of changes in the leaf-mesophyll tonoplast proteome in dependency of a cadmium exposure of barley (*Hordeum vulgare* L.) plants. Proteomics 2009;9:2668–77.
[30] Kieffer P, Dommes J, Hoffmann L, Hausman JF, Renaut J. Quantitative changes in protein expression of cadmium-exposed poplar plants. Proteomics 2008;8:2514–30.
[31] Kieffer P, Planchon S, Oufir M, Ziebel J, Dommes J, Hoffmann L, et al. Combining proteomics and metabolite analyses to unravel cadmium stress-response in poplar leaves. J Proteome Res 2009;8:400–17.
[32] Tuomainen MH, Nunan N, Lehesranta SJ, Tervahauta AI, Hassinen VH, Schat H, et al. Multivariate analysis of protein profiles of metal hyperaccumulator *Thlaspi caerulescens* accessions. Proteomics 2006;6:3696–706.
[33] Fagioni M, Zolla L. Does the different proteomic profile found in apical and basal leaves of spinach reveal a strategy of this plant toward cadmium pollution response? J Proteome Res 2009;8:2519–29.
[34] Roth U, von Roepenack-Lahaye E, Clemens S. Proteome changes in *Arabidopsis thaliana* roots upon exposure to Cd^{2+}. J Exp Bot 2006;57:4003–13.
[35] Alvarez S, Berla BM, Sheffield J, Cahoon RE, Jez JM, Hicks LM. Comprehensive analysis of the *Brassica juncea* root proteome in response to cadmium exposure by complementary proteomic approaches. Proteomics 2009;9:2419–31.
[36] Aloui A, Recorbet G, Gollotte A, Robert F, Valot B, Gianinazzi-Pearson V, et al. On the mechanisms of cadmium stress alleviation in *Medicago truncatula* by arbuscular mycorrhizal symbiosis: a root proteomic study. Proteomics 2009;9:420–33.
[37] Ombretta R, Gwénaelle B-C, Eliane D-G, Graziella B, Vivienne G-P, Silvio G. Targeted proteomics to identify cadmium-induced protein modifications in *Glomus mosseae*-inoculated pea roots. New Phytol 2003;157:555–67.
[38] Aina R, Labra M, Fumagalli P, Vannini C, Marsoni M, Cucchi U, et al. Thiol-peptide level and proteomic changes in response to cadmium toxicity in *Oryza sativa* L. roots. Environ Exp Bot 2007;59:381–92.
[39] Gil C, Boluda R, Ramos J. Determination and evaluation of cadmium, lead and nickel in greenhouse soils of Almeria (Spain). Chemosphere 2004;55:1027–34.
[40] Li J, Wu XD, Hao ST, Wang XJ, Ling HQ. Proteomic response to iron deficiency in tomato root. Proteomics 2008;8:2299–311.
[41] Ahsan N, Lee DG, Lee SH, Kang KY, Bahk JD, Choi MS, et al. A comparative proteomic analysis of tomato leaves in response to waterlogging stress. Physiol Plant 2007;131:555–70.
[42] Andaluz S, López-Millán AF, De las Rivas J, Aro EM, Abadía J, Abadía A. Proteomic profiles of thylakoid membranes and changes in response to iron deficiency. Photosynth Res 2006;89:141–55.
[43] Brumbarova T, Matros A, Mock HP, Bauer P. A proteomic study showing differential regulation of stress, redox regulation and peroxidase proteins by iron supply and the transcription factor FER. Plant J 2008;54:321–34.
[44] Kieffer P, Schroder P, Dommes J, Hoffmann L, Renaut J, Hausman JF. Proteomic and enzymatic response of poplar to cadmium stress. J Proteomics 2009;72:379–96.
[45] Fodor F, Gaspar L, Morales F, Gogorcena Y, Lucena JJ, Cseh E, et al. Effects of two iron sources on iron and cadmium allocation in poplar (*Populus alba*) plants exposed to cadmium. Tree Physiol 2005;25:1173–80.
[46] López-Millán AF, Morales F, Andaluz S, Gogorcena Y, Abadía A, De Las Rivas J, et al. Responses of sugar beet roots to iron deficiency. Changes in carbon assimilation and oxygen use. Plant Physiol 2000;124:885–98.
[47] Kováčik J, Klejdus B. Dynamics of phenolic acids and lignin accumulation in metal-treated *Matricaria chamomilla* roots. Plant Cell Rep 2008;27:605–15.
[48] Kováčik J, Klejdus B, Hedbavny J, Štork F, Bačkor M. Comparison of cadmium and copper effect on phenolic metabolism, mineral nutrients and stress-related parameters in *Matricaria chamomilla* plants. Plant Soil 2009;320:231–42.

[49] Laskowski MJ, Dreher KA, Gehring MA, Abel S, Gensler AL, Sussex IM. FQR1, a novel primary auxin-response gene, encodes a flavin mononucleotide-binding quinone reductase. Plant Physiol 2002;128:578–90.

[50] Chaffei C, Pageau K, Suzuki A, Gouia H, Ghorbel MH, Masclaux-Daubresse C. Cadmium toxicity induced changes in nitrogen management in *Lycopersicon esculentum* leading to a metabolic safeguard through an amino acid storage strategy. Plant Cell Physiol 2004;45:1681–93.